Title
ATOMIC SITE AND SPECIES DETERMINATIONS USING CHANNELLING AND RELATED EFFECTS IN ANALYTICAL ELECTRON MICROSCOPY

Author
Krishnan, K.M.

Publication Date
1986-10-01

LBL-22305
Preprint

Lawrence Berkeley Laboratory
UNIVERSITY OF CALIFORNIA

Materials & Molecular Research Division

Submitted to Ultramicroscopy

ATOMIC SITE AND SPECIES DETERMINATIONS USING CHANNELLING AND RELATED EFFECTS IN ANALYTICAL ELECTRON MICROSCOPY

K.M. Krishnan

October 1986

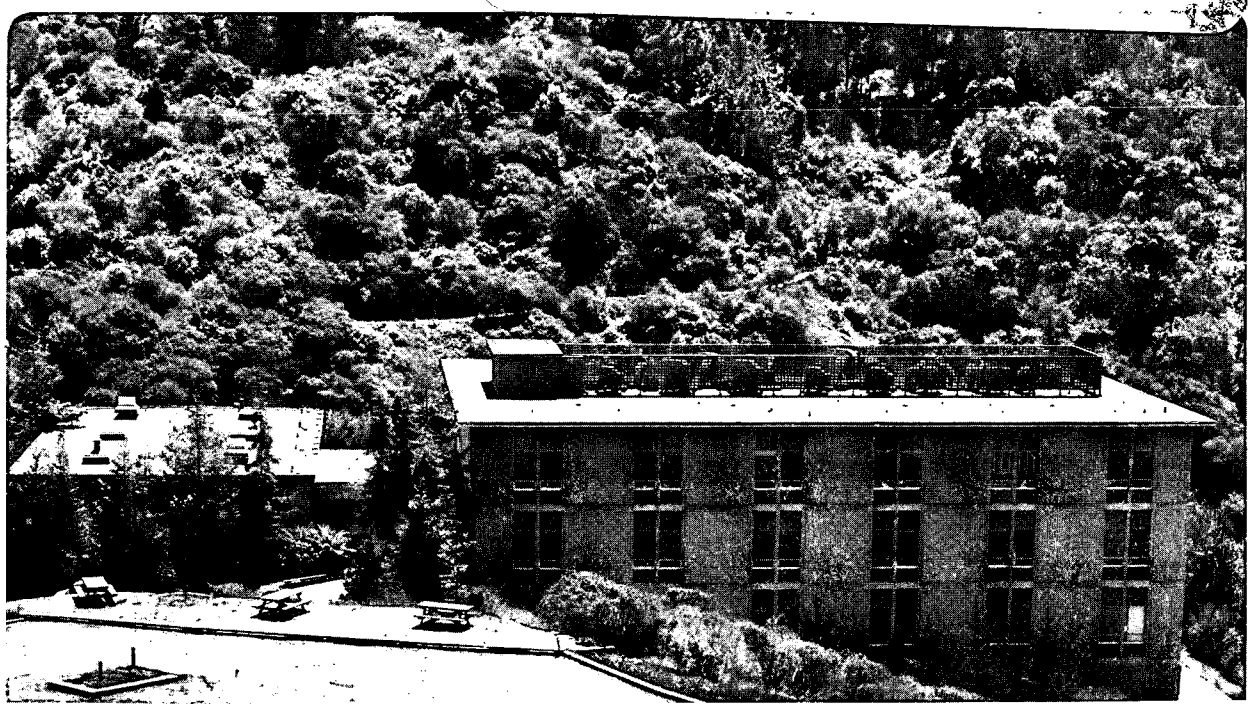

Prepared for the U.S. Department of Energy under Contract DE-AC03-76SF00098

DISCLAIMER

ATOMIC SITE AND SPECIES DETERMINATIONS USING CHANNELLING AND RELATED EFFECTS IN ANALYTICAL ELECTRON MICROSCOPY

Kannan M. Krishnan

National Center for Electron Microscopy
Materials and Molecular Research Division
Lawrence Berkeley Laboratory
Berkeley, California 94720, USA.

Submitted to ULTRAMICROSCOPY, Special Publication entitled " Limits of Submicron Spectroscopy ", edited by J. Hren and M. J. Kersker.

ATOMIC SITE AND SPECIES DETERMINATIONS USING CHANNELLING AND RELATED EFFECTS IN ANALYTICAL ELECTRON MICROSCOPY

Kannan M. Krishnan

National Center for Electron Microscopy
Materials and Molecular Research Division
Lawrence Berkeley Laboratory
Berkeley, California 94720, USA.

ABSTRACT

The formulation, development and applications of a novel crystallographic technique for specific site occupation determinations using the channelling or Borrman effect in electron diffraction is reviewed. This technique is based on the effect of incident beam orientations on the intensities of either the characteristic X-ray emissions or the characteristic energy-loss edges.

The formulation of the technique under planar-channelling conditions for simple layered structures (ALCHEMI - Atom location by channelling enhanced microanalysis) and a general formulation for non-layered structures, along with the relevant theory, are reviewed in detail.

In the case of characteristic energy-loss edges, in addition to being a function of the diffraction of the incident beam (channelling), the intensities are also a function of the diffraction of the outgoing inelastically scattered fast electron (blocking) and the scattering angle. A judicious choice of these parameters can provide additional information such as the specific site valence of a particular atomic species.

In general, this technique can distinguish neighbours in the periodic table; involves no adjustable parameters, external standards or special specimen preparations; is applicable to trace element concentrations (0.2 - 0.3 wt% or 10^{25} atoms/m^3); is very accurate ($\sim$3-10% error in site occupancy determinations, depending on the formulation used); and can be routinely applied at very high spatial resolutions ($\sim$10-40 nm).

Two crucial assumptions are made. The inelastic scattering events are assumed to be highly localized and the impurities/additions are assumed to be distributed uniformly with depth in the specimen.

These and other assumptions, limitations and possible improvements or extensions of the technique are discussed, but throughout the review, the emphasis is directed to practical considerations.

1. INTRODUCTION

The interactions of highly energetic charged particles, be they electrons, ions or positrons, with condensed matter, give rise to a wide variety of primary as well as secondary physical phenomena. These phenomena which include elastic scattering, energy-loss processes, secondary-electron emission and characteristic x-ray production, have cross-sections which depend on the nature of the localization of the scattering event (or the impact parameter) involved in their interactions with individual target atoms. In the case of amorphous materials where the atomic distribution is homogeneous and isotropic these impact parameters are independent of the relative orientation of the incident beam with respect to the target. Therefore the yields of these interaction processes, neglecting surface effects, are also orientation independent. For crystalline materials, at certain angles of incidence, the packing density of atoms will appear to be reduced because of the linear stacking of atoms and hence the probabilties or relative yields of these physical processes are also found to exhibit strong modulations with orientation. This effect is commonly referred to as " channelling " (see [1] for an extensive review).

This classical approach, though instructive, does not lend itself easily to a rigorous description of the

channelling phenomena in general and often a quantum mechanical description becomes necessary [2,3]. Which treatment is relevant is determined by the relativistic mass and the sign of the charge of the incident particle. For fast electrons accelerated through potentials of up to 300-400 kV the quantum mechanical or wave description is considered to be more accurate . However, at higher energies a classical description for the behaviour of fast electrons might be quite adequate [4]. In this wave model, the incident electron beam travelling through the crystal lattice is mathematically represented by a number of standing waves with the periodicity of the lattice. These standing waves known as Bloch waves [5] are sets of plane waves propagating through the crystal from the top surface with their wave front parallel to the surface normal. The probability of finding an electron at any point, or the local current density in a macroscopic sense, is given by the square of the amplitude of the Bloch wave at that point.

For certain incident beam orientations the modulation of the standing wave across the unit cell is such that its maxima coincides with the atomic positions. At these orientations, in addition to an enhanced absorption of the primary beam [6,7] due to inelastic excitation processes that are highly localized at atomic sites a correspondingly higher emisssion product would also be observed. For other orientations, the standing wave intensities would be a

minimum on these crystallographic sites with a concomitant reduction in absorption and emission products. This effect is also responsible for the anomalous transmission of X-rays as observed by Borrman [8] and later interpreted in a similar fashion by von Laue [9].

Hirsch, Howie and Whelan [10] suggested that the electron-induced characteristic X-ray emissions might also be dependent on the orientation of the incident beam, i.e. the "Borrman effect" might apply for the emission product. This was indeed observed by Duncumb [11] and further investigated by Hall [12] who confirmed that this effect was only of importance for thin crystals ($t \leq 200$ nm). Similar effects have also been observed for other secondary emissions such as cathodoluminescence [13]. Finally, in addition to a theoretical formalism to describe this phenomenon a comprehensive treatment of the orientation dependence of characteristic X-ray emission with particular emphasis on its ramification on conventional X-ray microanalysis has been developed [14].

Cowley [15] suggested that this absorptive effect in X-ray diffraction might contain structural information, particularly about the distribution of atoms in a diffracting crystal. The position of solute atoms in a crystalline lattice was experimentally determined by the nature of their X-ray fluoroscence during a diffracting

process by Batterman [16]. The techniques [17-22] of atomic site and species determination that are reviewed here are a logical extension of that work, the only difference being the use of incident fast-electrons instead of X-rays and the monitoring of either the secondary characteristic X-ray fluoroscence (EDXS) or the energy-loss electrons in transmission (EELS). In the latter case, there are more possibilities for the experimental arrangements as both the direction of incidence and collection can be selected independently. However, the interpretation of the orientation dependence of the characteristic energy-loss edges in transmission has to incorporate the multiple diffraction of the incident electron (channelling) and the outgoing inelastically scattered fast electron (blocking) [22].

2. BASIC PRINCIPLES OF CHANNELLING ENHANCED MICROANALYSIS

The characteristic X-ray case will be described first and this will be extended to the energy-loss case using the close relationship that exists between characteristic X-ray emissions and energy losses.

Fig. 1 shows the typical experimental arrangement in a conventional transmission electron microscope. The position of the detector with respect to the specimen is specified by the take-off angle (Ψ) which ranges from 20^0-70^0 depending

on the specific geometry of the particular microscope. In general, the higher the take-off angle the easier it is to perform the experiment as the detector geometry will not impose stringent restrictions on the available range of specimen tilts or incident beam orientations for optimal X-ray collection. The orientation of the incident beam with respect to the thin-foil specimen (θ) can be changed precisely by the use of a goniometer. One observes that the characteristic X-ray spectrum produced by the interaction of the fast electron with the specimen changes with orientation; intensities of individual peaks change but there is no change in peak positions as they correspond to specific atomic transitions (Fig. 2). Under certain favourable orientations, the X-ray spectra arising from beams maximized on specific crystallographic planes when compared to X-ray spectra arising from beams maximized between the same crystallographic planes can be used to obtain a microanalysis that is sensitive to the distribution of atoms on those planes. This, in principle, is the basis of Channelling Enhanced Microanalysis (CEM).

In order to be able to utilize this variation of X-ray intensities with orientation in the development of a meaningful technique of quantitative site occupancy determinations, it is essential not only to be able to determine these favourable orientations but also to obtain an independent measure of the electron intensity modulations

over the unit cell. In the case of X-ray incidence [16] the two-beam dynamical theory adequately describes the sinusoidal distribution of the X-ray standing wave over the crystal unit cell as well as the corresponding X-ray fluoroscence modulations. For electrons accelerated through kilovolt potentials, strong scattering may occur for passage of the radiation through only the first few atom-thicknesses of the crystal. This will give rise to many diffracted beams simultaneously even for a crystal thin enough to be considered a two-dimensional phase grating. In order to accomodate the multiple coherrent interactions of all these diffracted beams, the simple two-beam theory has to be replaced by a dynamical many-beam theory [23] for quantitative analysis. However, near the Bragg condition for a first order reflection, the two-beam theory does predict the correct qualitative trend for X-ray emission with orientation [18].

In some cases, the need for a theoretical prediction of the electron wavefield in the crystal can be avoided, by using the X-ray emissions from an atom whose distribution in the host crystal lattice is known. Any such emission can be used as a reference signal, and is proportional to the thickness averaged electron intensity on a specific crystallographic plane [17]. This is accomplished by performing these experiments in a systematic or " planar channelling " condition in which the crystal potential is

averaged in two orthogonal directions normal to the excited systematic row. Experimentally, this corresponds to the case when a single row of spots are seen in the transmitted electron diffraction pattern. For crystals with a layered structure (*i.e.* crystals that in some crystallographic projections can be resolved into alternating layers of parallel non-identical planes [A, B, A, B, ...], each plane containing one or more specific crystallographic site) the appropriate systematic row can be determined by mere inspection (Figs. 3a and 3b). For example, the spinel-structure compounds (Fig. 4) can be resolved in the [001] projection into alternating (400) planes of tetrahedral and octahedral sites and hence a g = 400 systematic row can be easily seen to be appropriate for this kind of experiment. Now, if an *a priori* knowledge of the distribution of some reference elements in the host lattice is available, their characteristic X-ray intensities could be used to obtain a measurement of the thickness averaged electron wavefield intensity on specific atomic planes. The distribution of impurity or alloying additions is then determined by an elegant method of ratios of their characteristic X-ray intensities with respect to those of the reference elements [17]. In many practical alloys/compounds (Fig. 5) it might not be possible to choose reference elements that are distributed uniquely on one and only one of the two alternating planes (Fig. 3b). Further, the alloying

concentrations might be large enough to significantly alter the distributions of the constituent elements in the original compound. In such case a more comprehensive formulation incorporating the stoichiometry of the original compound is required [19,24]. In the most general case (Fig. 3c), if the crystal structure is not layered, it is not easy either to determine the appropriate systematic orientation nor to monitor the electron wavefield using any of the secondary X-ray fluoroscence signals. In such cases, the electron-induced characteristic X-ray intensities for different site occupations and different incident beam orientations have to be calculated to determine the appropriate systematic or planar channelling condition prior to performing the experiment [20].

3. ATOM LOCATION BY CHANNELLING ENHANCED MICROANALYSIS (ALCHEMI)

This elegant method based on the above principles to detrmine substitutional or interstitial site occupancy of impurity atoms in layered structure compounds was originally formulated by Spence & Tafto [17]. In their formulation, two spectra under planar channelling conditions and a third spectrum under a random non-channelling orientation are required to perform the analysis. The planar-channelling condition or sytematic diffraction excitation is determined by inspecting the crystal structure as outlined in the

previous section. The random orientation is obtained by tilting the crystal to an orientation in which no lower-order Bragg diffraction vectors are excited (the no-Bragg case in Fig.2). However, the formulation is over-defined for the case that is treated in ref. [17] (*i.e.* for a crystal consisting of three elements : element a lying exclusively on the set of alternating planes A, element b lying exclusively on the other set of alternating planes B and the element x of unknown distribution, some fraction of which substitutes for element a on plane A and the rest substitutes for element b on plane B). Two orientations, a systematic and a random orientation are sufficient [25].

Let C_z be the fraction of element z on plane B, m_z the number of sites per unit cell for species z and P_z a factor that accounts for fluoroscence yield and other scaling factors. Here, z may be any of the elements a, b or x. Note that $C_a=0$ and $C_b=1$.

For any one particular planar-channelling orientation let I_A^1, I_B^1 be the depth-integrated electron intensity on the two planes A, B and N_z^1 be the observed characteristic X-ray intensity for the element z, where z may be a, b or x. Let I_A, I_B ($I_A = I_B = I$) and N_z be the corresponding terms for the non-channelling random orientation.

Then for the channelling orientation

$$N_a^1 = P_a\, m_a\, I_A^1 \tag{1}$$

$$N_b^1 = P_b\, m_b\, I_B^1 \tag{2}$$

$$N_x^1 = P_x\, m_x\, C_x\, I_B^1 + P_x\, m_x\, (1 - C_x)\, I_A^1 \tag{3}$$

and for the random orientation

$$N_a = P_a\, m_a\, I \tag{4}$$

$$N_b = P_b\, m_b\, I \tag{5}$$

$$N_x = P_x\, m_x\, I \tag{6}$$

from which one obtains

$$C_x = \frac{N_x^1/N_x - N_a^1/N_a}{N_b^1/N_b - N_a^1/N_a} \tag{7}$$

where C_x is the fraction of element x substituting for element b on the plane B.

The fast electron intensities do not appear in this final expression for atomic concentrations and hence it contains no adjustable parameters. Further, the dynamical wave field is used only as a variational parameter. Hence the precise orientation along the systematic row is unimportant and the thickness of the foil is not critical.

The results of ALCHEMI have been compared with other techniques and they are in good agreement [26]. Site occupancies for concentrations down to about 0.2 at% can be routinely detected by this method.

Even though the requirement of a layered structure (Fig. 3a) is a stringent one, this elegant formulation has found wide application. Ordering in minerals [27,28], site occupancy of impurity atoms in ceramic capacitors [29], point defects in compound semiconductors [30], alloying additions in superconducting materials [31], dopant site locations in semiconductors and the study of magnetic anisotropy [24,33] are some of the many problems that have been studied either by this method or by variations of it.

If the structure is layered but the requirement of the existence of at least one species that lies soley on one of the alternating planes is violated (Figures 3b & 5) more than one orientation along the same systematic row will be necessary to perform the analysis. The precise number of orientations required will then be determined by the stoichiometry of the original compound and the actual distribution of the reference elements before alloying [19]. However, this method would be unable to distinguish different sites within the same crystallographic planes. This limitation can be overcome by performing a series of experiments using linearly independent diffraction vectors. If it were possible to find three different sets of parallel planes in the crystal, experiments could be performed for each family of planes allowing complete determination of the occupation of any specific site in the structure. This experiment is yet to be performed !

4. A GENERALIZED FORMULATION

The formulation for the general case [20] will be reviewed now, where a projection of the crystal structure that separates the candidate sites for the impurities onto two planes each with a specific internal reference element cannot be found (Fig. 3c). The garnet structure (Fig. 6) with an average chemical formula of $A_3^{2+}[B_2^{3+}](Fe_3)O_{12}$, containing 160 atoms per unit cell and belonging to the space group I $4_1/a\ \bar{3}\ 2/d$ (O_h^{10}) is such a structure and will be used as an example. The appropriate planar channelling conditions cannot be determined by inspection nor can the characteristic X-ray intensities be used as a measure of the thickness averaged elctron intensities. Thus a theoretical prediction of electron wavefields in the crystal is necessary.

4.1 Theory

The derivation of an expression for characteristic X-ray production in thin crystals in the conventional dynamical theory formulation of electron diffraction [23] is reviewed here. Because of the strong interaction of fast electrons with matter, a two-beam theory would be an inadequate representation of the actual physical process.

The importance of many-beam interactions are well established [18].

It has been shown [34] that the incorporation of an imaginary crystal potential iP(r) in the Schrodinger equation

$$\nabla^2\phi + \frac{2m}{\hbar^2}(E + V + iP)\phi = 0 \qquad (8)$$

leads to a rate of energy loss per unit volume at the point r proportional to $P(r)\,|\phi(r)|^2$. The rate of "absorption" of electrons in a volume V is then given by

$$\frac{m}{hk}\int \bar{\nabla}\cdot\bar{s}\, d^3r = \frac{2m}{\hbar^2}\int P(\bar{r})\,|\phi(\bar{r})|^2\, d^3r \qquad (9)$$

and could approximate the characteristic X-ray production rate if P(r) is chosen appropriately.

The scattering proceses that lead to characteristic X-ray production in thin crystals are highy localized [20,35,36] and hence we assume that this imaginary part of the crystal potential is a delta function at the mean atomic prositions. Under this assumption, the rate of characertistic X-ray production given by eqn.(9) for any element z and crystal thickness t reduces to

$$N_z = \sum_{RCS}\int_0^t \phi^*\phi\, dz \qquad (10)$$

and the summation is over the relevant crystallographic sites (RCS) where the element z is distributed in the unit cell.

For an incident plane wave of electrons, the scattered wave amplitudes ϕ within the crystal can be expressed as a linear combination of Bloch waves [23]:

$$\phi(\bar{r}) = \sum_j \psi^j \sum_h C_h^j \exp[i(\bar{k}^j + \bar{h}).\bar{r}] \qquad (11)$$

where ψ^j are the excitation ampitudes of the j^{th} Bloch wave, $C_h{}^j$ are the Bloch wave coefficients and k_j are components of the wavevector for the electrons.

For centrosymmetric crystals, $\psi^j = C_o{}^j$. Neglecting absoprtion, one can then derive an expression for characteristic X-ray productions per unit thickness from eqns. (8)-(11) as:

$$N_z = \sum_{RCS} \sum_{g,h} \exp[i(\bar{h}-\bar{g}).\bar{r}] \sum_{j=l} C_o^{j*} C_g^{j*} C_o^l C_h^l + \sum_{j\neq l} C_o^{j*} C_g^{j*} C_o^l C_h^l \frac{\sin[(k^j - k^l)t]}{[(k^j - k^l)t]} . \qquad (12)$$

This expression for characteristic X-ray production is composed of two parts: a thickness-independent term of individual Bloch-wave contributions and a thickness-dependent term of Bloch-wave interference contributions. Thus a discussion in terms of the contribution of individual Bloch waves is misleading and erroneous [37]. Further, it

has been shown [20] that the contribution from the thickness-dependent term is small compared to the thicknes-independent term.

A detailed elaboration of this derivation is given elsewhere [20]. A similar treatment with the inclusion of absorption has been given by Cherns et al [37], and a more complete description of ionizing events in crystals including (e,2e) scattering kinematics has also been published [38].

4.2 Calculations

Results of the calculations [20] using the above theory for spinels and garnets is summarized here. The characteristic X-ray intensities calculated for Mg and Al in a normal spinel for a 15-beam (-7g to +7g), g=400 systematic excitation condition and over a range of incident beam orientation is shown in Fig. 7a. It can be seen that there is an enhanced emission for the octahedrally coordinated Al for negative excitation errors ($k_x/g < 0.5$) of the first order Bragg diffraction condition. The orientation dependence of the tetrahedrally coordinated Mg is reversed. These predictions are in good agreement with experimental results [40]. Similarly X-ray intensities were calculated [20] for complete occupation of all rare-earth elements in any one of the three crystallographic sites of a typical garnet structure compound $Y_3Fe_5O_{12}$ (YIG) for different

systematic or planar-channelling conditions (i.e., g=00$\bar{2}$, g=$\bar{2}$20, g=1$\bar{2}$1, etc.) in order to determine an orientation with specific-site sensitive characteristic X-ray emissions. A strong orientation dependence was predicted only for the g=1$\bar{2}$1 systematic row (Fig. 7b), i.e., enhancement for dodecahedral site substitutions of rare-earth elements, decrease in rare-earth X-ray signals for tetrahedral site substitution and an insensitivity to orientation for octahedral site occupations. Calculations for planar-channelling conditions using any other g vectors indicated that the emission product is insensitive both to site occupations and to incident-beam orientations.

4.3 Example of Experimental Applications

Specimens of YIG doped with small quantities of Samarium and Luticium additions used in the the experiment were prepared by routine ion-milling. Samples of 50nm thickness were used. Based on the calculations, a strong g=1$\bar{2}$1 systematic row was excited at 100 kV using a probe of 100 nm diameter, and characteristic X-ray spectra were collected at six different orientations of the incident electron beam:

(1) systematic orientation, $k_x/g=0$

(2) first-order Bragg diffraction with small negative excitation error ($s<0$); $k_x/g=0.375$;

(3) exact first-order Bragg diffraction; $k_x/g=0.5$;

(4) small negative deviation from the second-order Bragg diffraction; $k_x/g=0.875$;

(5) exact second-order Bragg diffraction; $k_x/g=1.0$

(6) second-order Bragg diffraction with small positive deviation parameter; $k_x/g=1.125$.

The specimens were oriented in all experiments using either convergent-beam electron diffraction or the Kikuchi-line method.

Normalized integrated elemental intensities for the two rare-earth additions Su, Lu are shown in Table I. The data is statistically significant but on inspection suggest that two provisional conclusions can be made: (a) the rare-earth additions of Sm and Lu predominantaly occupy the octahedral sites or (b) they are uniformly and evenly distributed between the dodecahedral and tetrahedral sites. This was resolved by calculating the probabilities of different site occupation determined by a least squares refinement based on a constrained least squares algorithm [41].

An error term was defined as the difference between the experimentally observed intensity and an intensity calculated as a summation over all sites of the product of the theoretical value for complete ocupation of each site and a weight factor representing the probability of occupation of that specific site. For each element of

interest, i.e., Sm and Lu, a summation over all orientations of the square of this error term was minimized, subject to the constraint that all the weights were positive. The results of the least squares refinement for the weights of the occupation for each element in a particlar site is shown in Table II.

Within the limitations of the assumptions of the technique, it can be inferred that the small rare-earth additions tend to occupy the octahedral sites with a probability >95%. This is in good agreement with earlier studies [42,43].

This generalized method can be applied to all crystal structures, as long as a planar-channeling condition that is crstallographic site sensitive can be determined by the calculations. The calculations are only an approximation of the physical process and in general this method will produce larger errors compared to the elegant ALCHEMI formulation where the need to calculate electron wavefields has been eliminated by using the known distribution of certain elements as an internal reference. In general then, each problem of site occupancy has to be tackled separately, beginning by classifying the crystal structure into one of the three categories shown in Fig. 3, and proceeding with the appropriate formulation reviewed above.

Finally, even though these experiments are performed at a fixed acceleration voltage, recent studies [51,52] indicate that there is a significant effect of the acceleration voltage as an independent parameter on the orientation dependence of characteristic X-ray production in thin crystals. The combined effect gives rise to an interesting phenomenon termed as the "inversion voltage" which is characterized by a change in the sign of the orientation dependence. This "inversion voltage" has been shown to be different from the conventional critical voltage effect. In principle, this effect has no direct consequence on any of the formulations reviewed above. However, more work needs to be done to obtain a true understanding of this phenomenon.

5. AXIAL ELECTRON CHANNELLING ANALYSIS

For monoatomic crystals containing very small quantities of dopants - a case quite common in semiconductor applications, independent reference signals from distinct species known to occupy specific sites is not available. In such cases, absolute X-ray yields for both the host and impurity atoms need to be measured to determine either the site occupancies or the fraction of impurity atoms occupying substitutional sites. This requires very high instrument stability as has been well demonstrated in the study of a

high purity single crystal silicon with 3 x 10^{25} atoms/m^3 of arsenic dopant concentration [32].

However, the orientation dependence of characteristic X-ray production is much higher in the zone axis orientation compared to the planar channelling condition [50,55]. This is illustrated in Fig. 8, from which it can be concluded that there is an increase in sensitivity by at least a factor of two over the planar channelling arrangement. If one is interested in determining whether the dopant is substitutional or interstitial, it is possible to determine the fraction of the substitutional dopant for even smaller concentrations by successive measurements along two or more different axial-channelling conditions [50]. Further, if the dopant is assumed to be uniformly distributed, a simple ratio method of host and impurity X-ray measurements has been formulated, thus eliminating any need for either calculating the elctron wavefields or measuring absolute X-ray intensities, to determine the degree of substitution [55].

This method is sensitive to localization effects and appropriate corrections are necessary. Further, it is difficult to separately resolve a candidate site on a specific crystallographic plane in the axial channelling orientation and hence this method is not applicable to as

wide a range of problems as the planar-channelling formulation.

6. ENERGY LOSSES FROM CHANNELLED ELECTRONS

In principle, characteristic energy loss edge intensities and the corresponding characteristic X-ray emissions should show identical variation with incident-beam orientation. The only difference is a constant term, the fluorescence yield. However, there are two other important factors to be considered [44,22].

The characteristic X-ray emissions are isotropic. Therefore the detector position is important only to the extent that it determines the signal to background ratios and is of no consequence as far as these types of channelling experiments are concerned. However, for energy losses that are relevant in analytical electron microscopy, using incident electrons accelerated through 100-300 kV, the principle of reciprocity [45] can be applied to a good approximation, as long as the situation is restricted to the single scattering regime and plural scattering is avoided. In simple terms, this principle states that an interchange of source and detector gives the same results. It can be argued that if a change in incident beam orientation produces a change in the localization of the electron wavefield on the different crystallographic sites, then

detecting the inelastically scattered electrons in different directions should also produce a greater or lesser characteristic energy-loss intensity for elements occupying the same sites. Resorting to this principle, the sensitivity of EELS to different site occupation can be effectively squared by choosing the position of the detection aperture and placing it at an appropriate part of the diffraction pattern to be energy analyzed [46].

The other factor is the "localization" of the corresponding inelastically scattered event. It can be readily understood from a simple application of the uncertainty princple ($\Delta x * \Delta p \geq h$) that the distance a fast electron can pass from the atom in a crystal and still ionize it, is inversely proportional to the momentum exchange associated with the inelastic scattering event. Simple calculations [44] show that for a 100 keV incident beam, energy losses $\geq$ 2 keV can be considered to be sufficiently localized even in the forward direction, but for losses smaller than 1 keV the localization is insufficient and the information contained might be averaged over a number of different crystallographic sites. However, by analyzing electrons scattered over large angles (i.e., large momentum exchange), the specific site sensitivity can be greatly increased even for 500 eV loss electrons as the corresponding inelastic scattering event would be more

localized. This enhancement of site selectivity is similar to double alignment in particle channelling [47].

The diffraction geometries and the EELS spectra obtained with the incident wavefield preferentially localized on the octahedral site (a) and tetrahedral sites (b) in a prototype spinel $MgAl_2O_4$ compound are shown in Figs. 9 and 10. In Fig. 10 the localization is considerably enhanced by selecting only large angle scattering events - a demonstration of this channelling and blocking effect.

The much better energy resolution of EELS, ~1-2 eV for an analytical electron microscope using a LaB_6 filament, compared to EDXS (~150 eV for Mn K_α radiation) makes it possible to perform specific site valence state determinations using the chemical shift due to a particular change in valence. For example, using the 2 eV chemical shift between Fe^{3+} and Fe^{2+} observable in EELS, and applying this method it has been shown [21] that Fe^{3+} occupy octahedral sites while Fe^{2+} occupy tetrahedral sites in a naturally occurring chromite spinel (Figs. 11 and 12).

In spite of the possibility of obtaining this additional information, it must be cautioned that in general, X-ray emission is to be preferred over EELS to perform these channelling experiments because of better fractional sensitivity.

It is also possible to obtain crystallographic information such as the nearest neighbour environment of a particular atomic species from the extended energy loss fine structure (EXELFS). However, this method requires the use of adjustable parameters in addition to elaborate data reduction processes. Even then such information as quantitative site occupancy cannot be obtained. Further, the long range oscillations associated with EXELFS are weak, and in most practical applications, the technique is impaired by overlaps of the characteristic energy-loss edges of interest.

6. DISCUSSION

An underlying assumption in all these formulations is that the inner shell excitation processes associated with both characteristic X-ray emissions and energy losses are highly localized. Estimating the time over which a virtual photon is exchanged between a fast electron of velocity v and the excited particle, converting that using the uncertainty principle [36] and using a number of radically simplified arguments, a limiting value of the associated impact parameter, b, has been derived [35] as:

$$\langle b \rangle = 1.24\ hv\ /\ 4.46E_c \qquad (13)$$

where E_c is the initial energy for the onset of the transition. Some representative values of the impact

parameter calculated using this expression are given in Table III. Alternatively, for highly localized inner-shell excitations, the inelastic potential is well approximated by a delta function $\delta(r)$, such that its Fourier transform P_{gh} is a constant. This implies that the momentum transfer q of the incident electron is such that $q >> g,h$. The minimum momentum transfer for the onset of the transition is given by the expression $q_{min} = k\ (\Delta E/2T)$ and can be shown to satisfy the above criterion, for the X-ray emissions of the rare-earth elements discussed in this paper [20]. Irrespective of whether this discussion of localization is made in real space or in reciprocal space, it can be concluded that the error introduced in occupancies by localization effects is not greater than 2-3 %.

It is often believed that the spatial resolution of these channelling techniques is limited by the need for "parallel" illumination because of the considerable reduction in this characteristic X-ray production anamoly when "non-parallel" illumination is used. In practice a spatial resolution of 10-40nm has been routinely achieved and it seems that the "parallel" illumination criterion can be met by ensuring that the illumination semi-angle is not larger than the Bragg angle for the first order reflection. However, in some cases (Fig. 3b) independent measurements have to be made at several closely spaced orientations. Recent results [48,49] indicate that the beam is most

parallel when focussed on the specimen plane. This is an inherrent feature in most modern microscopes where the objective is an immersion lens and the electrons follow a helical path. Hence, a beam that has substantial convergence is to be preferred over a conventional/apparent "parallel" beam (sharp diffraction spots in the back focal plane) to perform these channelling experiments. This is another area that needs to be studied in greater detail.

The spatial resolution is also determined by the statistics of the energy dispersive X-ray detection process. A uniform distribution of impurities, in sufficiently large numbers under the electron probe to provide an adequate sampling is required. It is estimated that reasonable results can be obtained using a 20nm probe for a 10^{25} atoms m^{-3} distribution of impurities in a large unit cell crystal. In general the condition that has to be satisfied [17] in order that the dynamical wavefunction is well sampled in depth is given by

$$\xi_g \, n \, A \geq 1 \qquad (14)$$

where n(atoms/unit volume) is the uniformly distributed concentration, A is the projected area of the electron probe and ξ_g is the dynamical extinction distance for the reflection g. Further, since all intensities are thickness averaged, the distribution of impurities in the crystal should be uniform with depth and hence problems where there

are layers of impurities perpendicular to the foil normal are to be avoided. The quality of the crrystal or the degree of disorder in the alloy that is amenable to study by this method is best judged by the presence of sharp features in the transmitted Kikuchi line pattern.

There are no special specimen preparation requirements; both routine ion-milled samples or crushed samples can be used. Normally, stray X-ray generation can be mimized by using gridless self-supporting samples that are thin throughout their area. On the other hnd, it can also be argued that a small amount of material on a grid gives less. spurious effects than a self-supporting specimen. A discussion of this subject is very subjective, as there are no detailed studies of spuriosities in an analytical transmission electron microscope.

Normally, the optimal thickness to be used depends on the absorption parameters and the extinction distance corresponding to the dominant Bragg reflection. A reasonable starting value is about one extinction distance and often an optimum value of the thickness can be selected by observing the appearance of Kikuchi line contrast (which also results from a thickness averaged bulk localized scattering process). However, there is an upper limit of thickness (approximately 3 extinction distances) corresponding to the attenuation distance for the poorly transmitted Bloch

waves. At distances greater than this the electrons are diffusely scattered through small angles and effectively behave as plane waves in producing further X-rays.

Any bending or thickness changes under the probe are unimportant as both the impurity as well as the reference elements are affected in the same way by any local change in orientation.

The technique that has been described is subject to all the limitations of conventional energy dispersive X-ray microanalysis and hence is limited to the analysis of elements with atomic number $Z \geq 11$ unless windowless or ultra-thin window detectors are used. However, UTW detectors (particularly in the JEOL microscopes) are placed at a take-off angle of 0^0 (i.e., horizontal, in the specimen plane) and the specimen has to be tilted by $40\text{-}45^0$ for optimal X-ray collection. To accommodate this specimen-detector geometry, single crystal specimens must be cut such that the foil normal is approximately $40\text{-}45^0$ away from the zone-axis of interest. In general, it is best to use EELS for low atomic number elements. However, the detection aperture has to be positioned appropriately, taking into consideration both the localization as well as the channelling and blocking effects (described in Section 5), such that the signal is maximized.

The ramificatons of this effect on conventional X-ray microanalysis is discussed in great detail elsewhere [37]. It suffices to say, that no significant errors would be observed either if a very large illumination aperture is used or if the specimen is systematically tilted to an orientation such that no lower order Bragg diffraciton vectors are excited [52].

These techniques of planar-channelling are capable of resolving adjascent elements in the Periodic Table and site occupations of trace-elemental compositions (0.2-0.3 wt%) can be routinely determined. The error in the ALCHEMI formulation for site occupancy determination is on an average about $\pm$ 3 %. In the generalized formulation the smallest error in the fraction of the total concentration occupying a particular site is a compounded one consisting of the inherrent approximations of the theoretical formulations, the statistical error in experimentation and the computational error in last squares refinements. Hence, the smallest error achievable is greater and is estimated to be about $\pm$ 5-10 %.

Even though the results of ALCHEMI agree very well with those of other techniques such as X-ray diffraction, it has significant advantages over any other method of site occupancy determinations. X-ray diffraction and Rutherford back scattering cannot distinguish adjacent elements in the

Periodic Table while EXAFS/EXELFS and HREM require adjustable parameters. In some cases ion and electron channelling experiments are complementary [50], ion channelling experiments have good depth resolution but poor lateral resolution (order of millimeters), whereas electron channelling measurements are thickness integrated but with nanometer scale lateral resolution.

The techniques discussed in this review are limited to the study of radiation insensitive materials. In some cases, where the material is susceptible to ionization damage, performing these experiments at higher acceleration voltages would yield better results. However, the experiments should be performed at a fixed acceleration voltage only, as the combined effects of acceleration voltage and incident beam orientation gives rise to interesting effects such as the " inversion voltage " that are not yet well understood. The use of a higher brightness source such as a field emission gun would, in principle, considerably improve the lateral spatial resolution of these techniques.

The detection limits in the planar-channelling case (10^{25} atoms m^{-3}) must be improved to make these techniques amenable to other applications, particularly in semiconductor materials characterization. It has been suggested [53] that poor signal to noise limitations could be overcome by coincidence measurements of characteristic X-ray emissions and characteristic energy losses. Recent

developments in parallel detection instrumentation for electron energy loss spectroscopy [54] could provide the necessary impetus for these measurements. Counting time limitations (in the application to radiation sensitive materials) due to pulse pile-up of X-rays from the matrix could also be overcome using appropriate filters to suppress the matrix X-ray counts.

ACKNOWLEDGEMENTS

This work was supported by the Director, Office of Energy Research, Office of Basic Energy Sciences, Materials Sciences Division of the U.S. Department of Energy under Contract No. DE-AC03-76SF00098.

The author would like to thank Prof. G.Thomas for his constant encouragement and support, Dr. P.Rez for many stimulating discussions on the subject and Drs. J. Tafto, J. C. H. Spence, O. L. Krivanek and S. J. Pennycook for permission to use some of their previously published results.

Table I

Normalized integrated elemental intensities [20]

K_x/g	0	0.375	0.5	0.875	1.0	1.125
Lu(Lα)	50807	49747	49130	50142	48985	50437
Sm(Lα)	31911	31754	31808	32073	31218	31805

Table II

Relative weights for rare-earth site occupancies [20]

	Octahedral	Tetrahedral	Dodocahedral
Lu	0.2141±0.02	0.0049±0.0005	**
Sm	0.1679±0.0164	**	0.0095±0.0007

Table III

Expectation values for the impact parameter <b>

Emission	E_c(keV)	<b> (nm)
Al Kα	1.486	0.0231
Mg Kα	1.253	0.0274
Sm Lα	6.656	0.0068
Lu Lα	9.281	0.0037

REFERENCES

[1] Donald S. Gemmell, Rev. Mod. Phys. 46 (1974) 129.
[2] L. T. Chadderton, Channelling, ed., D. V. Morgan (Wiley, London, 1973) p. 287.
[3] K. Komaki and F. Fujimoto, Phys. Lett. 58A (1981) 51.
[4] M. V. Berry, B. F. Buxton and A. M. Ozorio de Almeida, Radiation Effects 20 (1973) 1.
[5] C. Kittel, Introduction to Solid State Physics, 6th ed., (Wiley, New York, 1986)
[6] G. Honjo, J. Phys. Soc. Jpn, 8 (1953) 776.
[7] H. Hashimoto, A. Howie and M. J. Whelan, Phil. Mag. 5 (1960) 967.
[8] G. Borrman, Phys. Z. 42 (1941) 157.
[9] M. von Laue, Acta Cryst. 2 (1949) 106.
[10] P. B. Hirsch, A. Howie and M. J. Whelan, Phil. Mag. 7 (1962) 2095.
[11] P. Duncumb, Phil. Mag. 7 (1962) 2101.
[12] C. R. Hall, Proc. R. Soc. Lon. Ser A295 (1966) 140.
[13] S. J. Pennycook and A. Howie, Phil Mag. A41 (1980) 809.
[14] D. Cherns, A. Howie and M. H. Jacobs, Z. Naturforsch. Teil A28 (1973) 565.
[15] J. M. Cowley, Acta Cryst. 17 (1964) 33.
[16] B. W. Batterman, Phys. Rev. Lett 22 (1969) 703.
[17] J. C. H. Spence and J. Tafto, J. Microsc. 130 (1983) 147.
[18] J. C. H. Spence and J. Tafto, SEM/II (1982) 523.
[19] K. M. Krishnan and G. Thomas, J. Microsc. 136 (1984) 97
[20] K. M. Krishnan, P. Rez and G. Thomas, Acta Cryst. B41 (1985) 396.
[21] J. Tafto and O. L. Krivanek, Phys. Rev. Lett. 48 (1982) 560.
[22] J. Tafto and O. L. Krivanek, Nuc. Inst. Meth. 194 (1982) 153.
[23] P. B. Hirsch, A. Howie, R. B. Nicholson, D. Pashley, and M. J. Whelan, Electron Microscopy of Thin Crystals (Butterworths, London, 1965).
[24] K. M. Krishnan, L. Rabenberg, R. K. Mishra and G. Thomas, J. Appl. Phys. 55 (1984) 2058.
[25] E. Goo, Appl. Phys. Lett. 48 (1986) 1779.
[26] J. Tafto & P.R. Busek, Amer. Min. (1982).
[27] J. Tafto & J.C.H. Spence, Science, 218 (1982) 49.
[28] P.G. Self & P.R. Busek, EMSA Proc. 41 (1983) 178.
[29] H.M. Chan, M.P. Harmer, M. Lal and D.M. Smyth, Mat. Res. Soc. Symp. Proc. 31 (1984) 345.
[30] Z. Liliental, J. Appl. Phys. 54 (1983) 2097.
[31] J. Tafto, R.L. Sabatini & M. Suenaga, EMSA Proc. 43 (1985) 196.
[32] J. Tafto, J.C.H. Spence and P. Fejes, J. Appl. Phys. 54 (1983) 5014.

[33] K.M. Krishnan, P. Rez, R. Mishra & G. Thomas, Mat. Res. Soc. Symp. Proc. 31 (1984) 79.
[34] R.D. Heidenreich, J. Appl. Phys. 33 (1962) 2321.
[35] A.J. Bourdillon, P.G. Self and W.M. Stobbs, Phil. Mag A44 (1981) 1335.
[36] A. Howie, J. Microsc. 117 (1979) 11.
[37] D. Cherns, A. Howie and M.H. Jacobs, Z. Naturforsch. Teil A28 (1973) 565.
[38] V.W. Maslen and C.J. Rossouw, Phil. Mag. A47 (1983) 119.
[39] S. Geller and M.A. Gilleo, Acta Cryst. 10 (1957) 239.
[40] J. Tafto and J.C.H. Spence, Ultramicroscopy 9 (1982) 243.
[41] C.L. Lawson and R.J. Hanson, Solving Least Squares Problems, Ch. 23 and 25 (Prentice-Hall, New Jersey, 1974).
[42] L. Suchow & M. Kakta, J. Sol. Stat. Chem. 5 (1972) 329.
[43] S.L. Blank, J.W. Nielsen and W.A. Biolsi, J. Elec. Chem. Soc. 123 (1976) 856.
[44] O.L. Krivanek, M.M. Disko, J. Tafto and J.C.H. Spence, Ultramicroscopy 9 (1982) 249.
[45] J.M. Cowley, Appl. Phys. Lett. 15 (1968) 58.
[46] J. Tafto and O.L. Krivanek, EMSA Proc. 39 (1981) 190.
[47] S.T. Picraux, W.L. Brown and W.M. Gibson, Phys. Rev. B6 (1972) 1382.
[48] K.K . Christenson and J.A. Eades, EMSA Proc. 44 (1986) 622.
[49] K.K. Christenson and J.A. Eades, Ultramicroscopy 19 (1986) 191.
[50] S.J. Pennycook. J. Narayan and O.W. Holland, Appl. Phys. Lett. 44 (1984) 547.
[51] K.M. Krishnan, P. Rez and G. Thomas, Proceedings of the 7th International HVEM Conference, ed., R. Fisher, R. Gronsky and K.H. Westmacott (1983) 365.
[52] K.M. Krishnan, P. Rez, G. Thomas, Y. Yokota & H. Hashimoto, Phil. Mag. 53 (1986) 339.
[53] D. Wittry, Ultramicroscopy 1 (1976) 297.
[54] O.L. Krivanek, C.C. Ahn and R.B. Keeny, Preprint.
[55] S. J. Pennycook and J. Narayan, Phys. Rev. Lett. 54 (1985) 1543

Figure Captions

Fig. 1. Physical principles of channelling enhanced microanalysis. (a) the epxerimental arrangement. (b) the projected crystal structure with the standing-wave pattern of the primary beam set up as a result of the dynamical scattering. For a systematic orientation the wavefield is two-dimensional (i.e., constant in a direction normal to the page). The modulation of the standing wave on specific crystallographic planes is then a function of the incident-beam orienation. (c) Highly localized secondary phenomena such as characteristic X-ray emissions are also a function of these modulations of the pimary beam. For the favourable orientation the Bloch waves are maximized on the A planes with a concomitant increase for the elements occupying the sites △. For the other favourable orientation, the maximization is on the B planes with a corresponding increase for the elements occupying the sites **O** . By monitoring these orientation-dependent emission products and resorting to the anlyses to be reviewed in this paper, specific site occupations can be quantitatively determined.

Fig. 2 A typical set of energy-dispersive X-ray spectra for $MgAl_2O_4$ (spinel) as a function of indcident beam orientation. " Parallel illumination " conditions were used. The precise orientation of each acquisition is shown in the insets. Notice the wide range in the ratio of the X-ray intentsities for the two cations Al and Mg.

Fig. 3. Hypothetical two-dimensional figures illustrating the classificaiton of crystal strucutres in this review. The distribution of the crystallographic sites of interest □, **O** determine whether the structure is layered [(a) and (b)] or not [(c)]. If the distribution of the reference elements a, b are known *a priori*, a planar-channelling orientation and a random orientation are sufficient to perform the analysis for the simplest case [(a)]. In the general case, where the distribution of the reference elements are not well defined [(c)], the characteristic X-ray emissions have to be calculated and refined using a constrained least-squares method to determine site occupancies.

Fig. 4 A [001] projection in perspective of the spinel structure (2x2x2 unit cells are shown). Mg and Al positions in the structure are represented by squares and triangles respectively. Notice that the structure is layered. (courtesy P. Stadelman).

Fig. 5 Hexagonal Sm_2Co_{17} primitive unit cell along with the corresponding primitive cell of the $SmCo_5$ structure. This structure is layered and contains alternating (0001) pure Co and mixed Sm-Co planes. Substitution of transition metal additions for Co in the dumbbell sites is of interest in magnetic applications.

Fig. 6 The cation arrangement in the garnet structure. Only half the unit cell bereit of the oxygen atom is shown. The octahedral sites [a] form a repeating b.c.c. strucutre with a lattice parameter $a_0' = a_0/2$ [39].

Fig. 7(a) Results of the orientation-dependent X-ray emision calculation for spinels. A 15-beam, g=004 systematic excitation condition and a specimen thickness of 10 nm were the conditions used. The orientation of the incident beam was specified by varying the excitation error (k_x/g) which is defined such that $k_x/g = 0.5$ for the exact first-order Bragg diffraction condition.

Fig. 7(b) Calculated orientation dependence of the characteristic X-ray emissoins for the garnet structure. An 11-beam (-5g to +5g), g=121 systematic excitation condition and two thickness (25, 50 nm) were the conditions used. Notice the change in scale of the intensity for octahedral site substitutions.

Fig. 8 X-ray emission spectra obtained from a sample of Silicon doped with Antimony in the (220) planar (a,b), the <100> axial (c,d) and the <111> axial (e,f) channelling orientations. The increased sensitivity in the axial orientation can be used to extend the channelling enhanced microanalysis method to lower concentrations of impurities. However, only the level of substitution on crystallographic planes or interstitial occupation can be easily resolved [55].

Fig. 9 EEL spectra of spinel under channelling conditions but with poor localization. The illuminating and detector apertures overlap and their position relative to the (400) and (800) Kikuchi lines are also shown. Notice the poor channelling and/or blocking irrespective of whether the octahedral sites (a) or tetrahedral sites (b) are selected [22].

Fig. 10 EEL spectra of spinel, collected under conditions identical to Fig. 9. In this case, the detection apertures were shifted parallel to the (400) Kikuchi band such that only the high angle scattered electrons wre detected but without any change in the diffraction geometry with respect to the (400) planes. Significant enhancement for oxygen K-edge at 530eV and moderate enhancement for Aluminum K-edge at 1560eV and Magnesium K-edge at 1305eV with orientation are now clearly evident [22].

Fig. 11 EEL spectra of a chromite spinel measured at differnt incident beam orientations and under strong localization conditions. Selective enhancement of octahedral sites (a) and tetrahedral sites (b) can be observed.

Fig. 12 Details of the Fe $L_{2,3}$ edge for the same orientations shown in Fig. 11. Notice the 2 eV chemical shift between the Fe^{2+} and the Fe^{3+} with the the Fe^{3+} at higher energy. The higher energy Fe^{3+} peak is also enhanced at an orientation in which the electron beam is localized on the octahedral sites, identical to the behaviour of the oxygen and chromium characteristic energy loss edges [21].

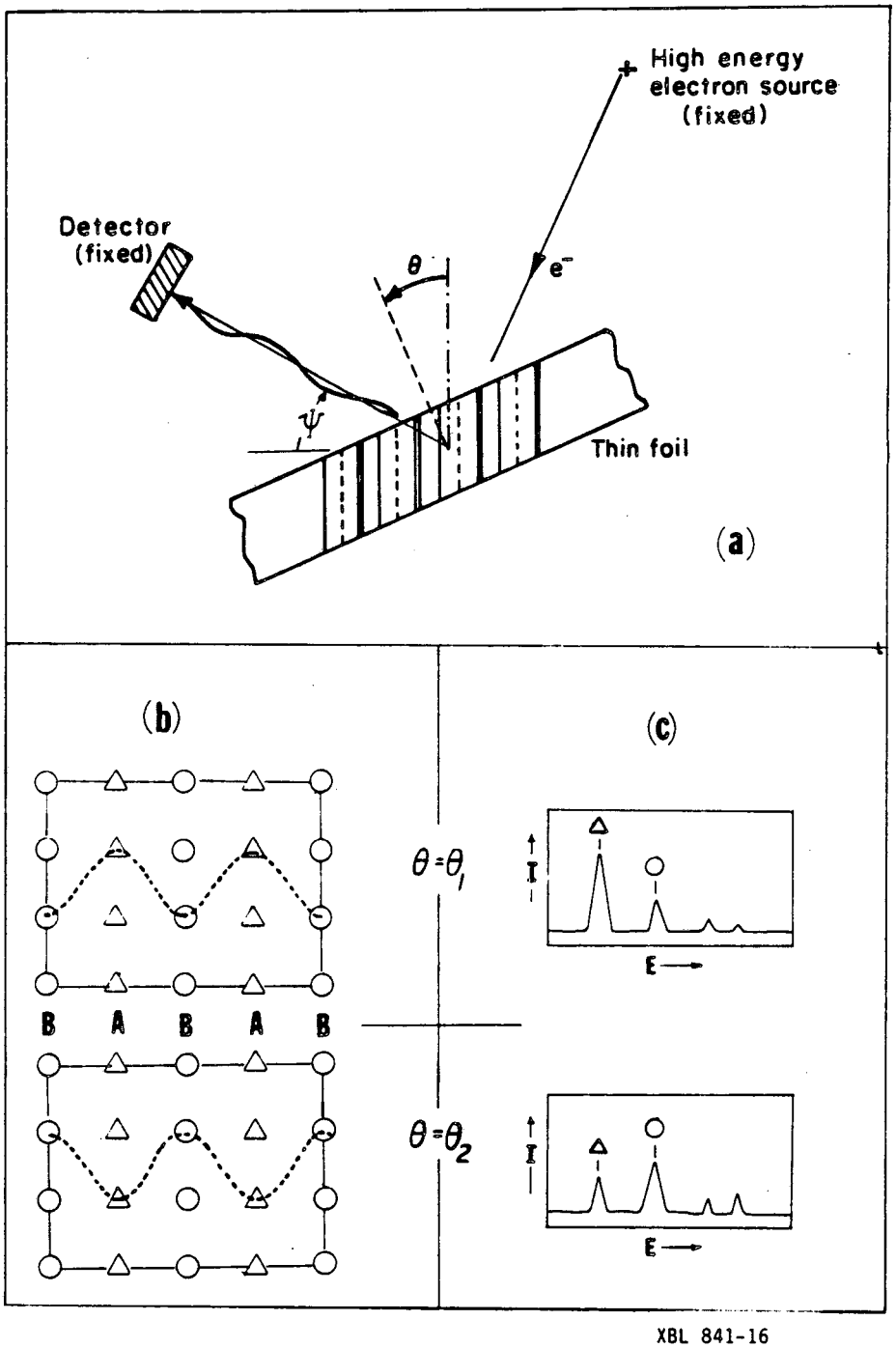
High energy
electron source
(fixed)
Detector
(fixed)
θ
e⁻
ψ
Thin foil
(a)
(b)
(c)
B A B A B
θ=θ1
θ=θ2
I
E
XBL 841-16

Fig. 1

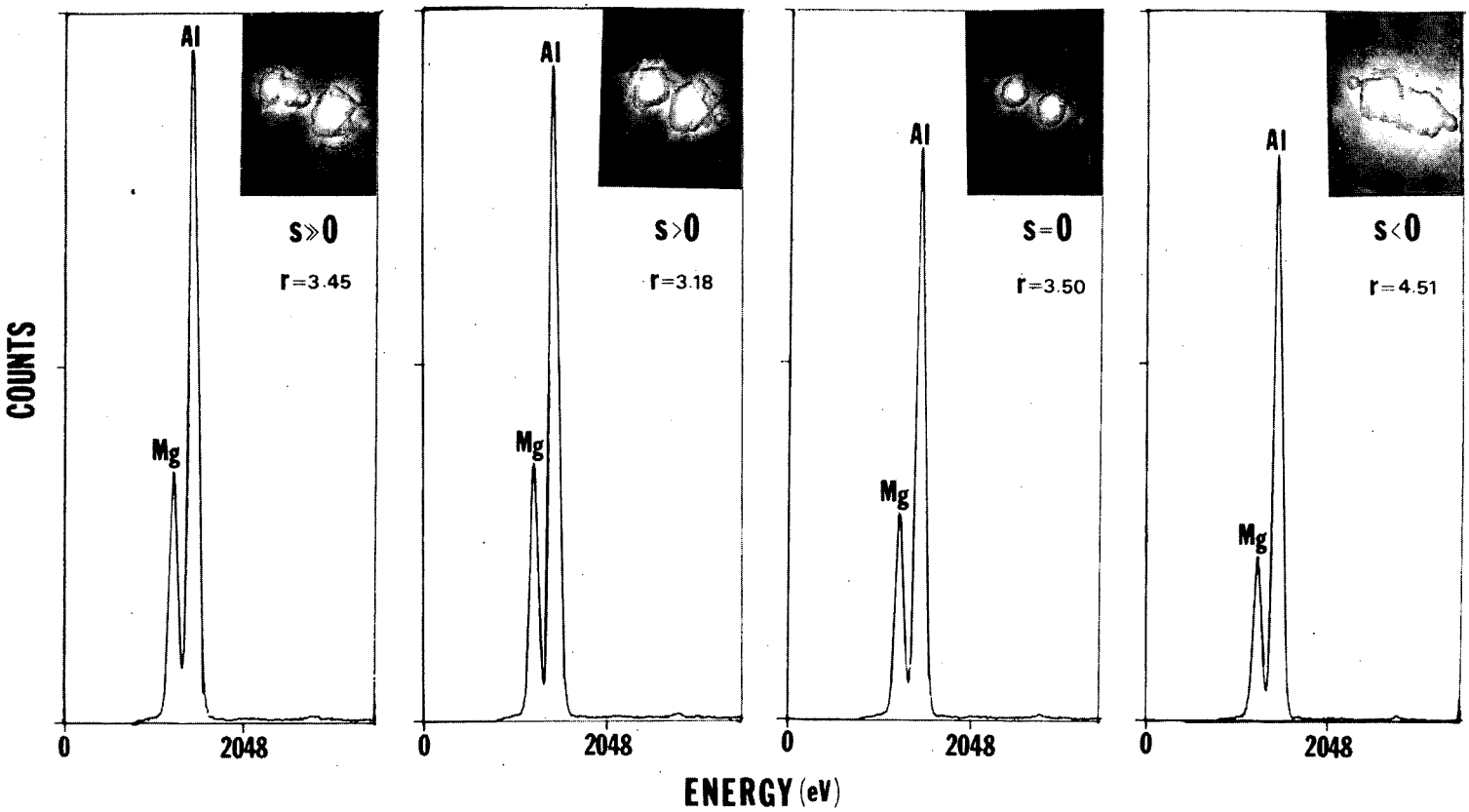

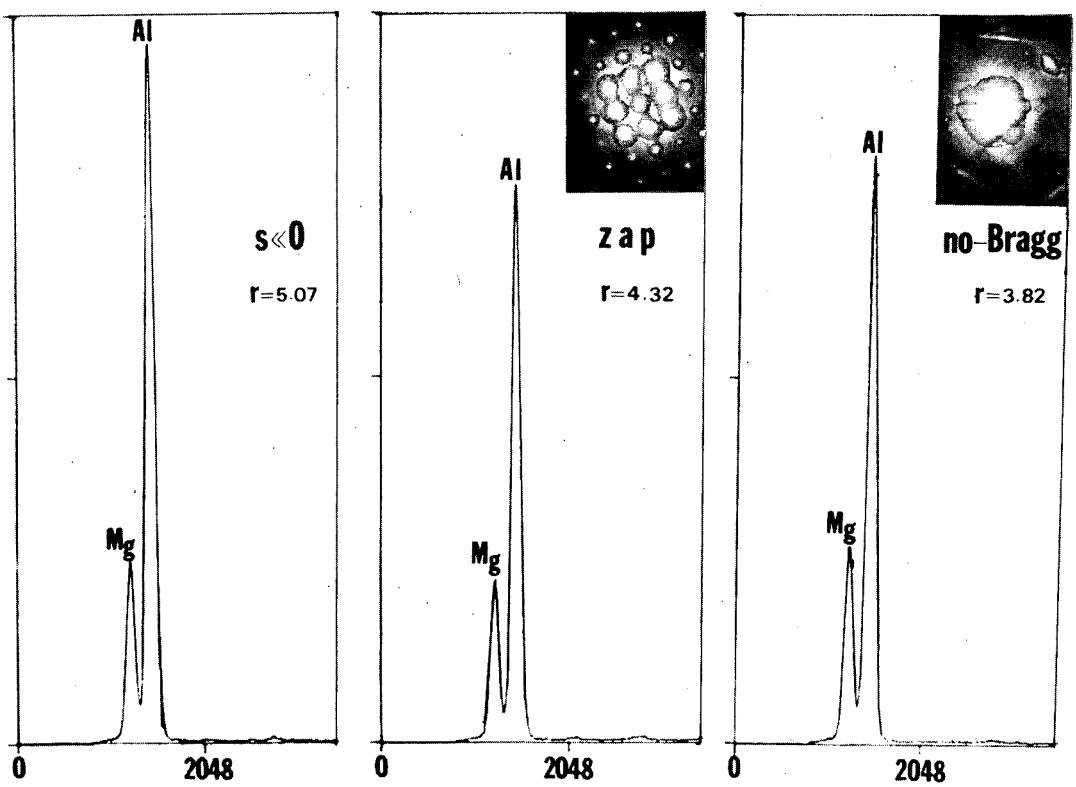

$MgAl_2O_4$

300 Kv

$r = N_{Al}/N_{Mg}$

Fig 2

XBB 855-3698

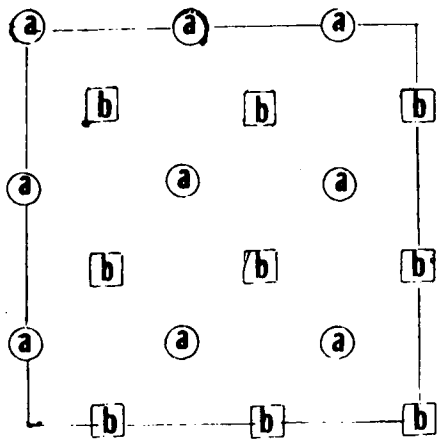

XBL 8310-12160

Fig. 3

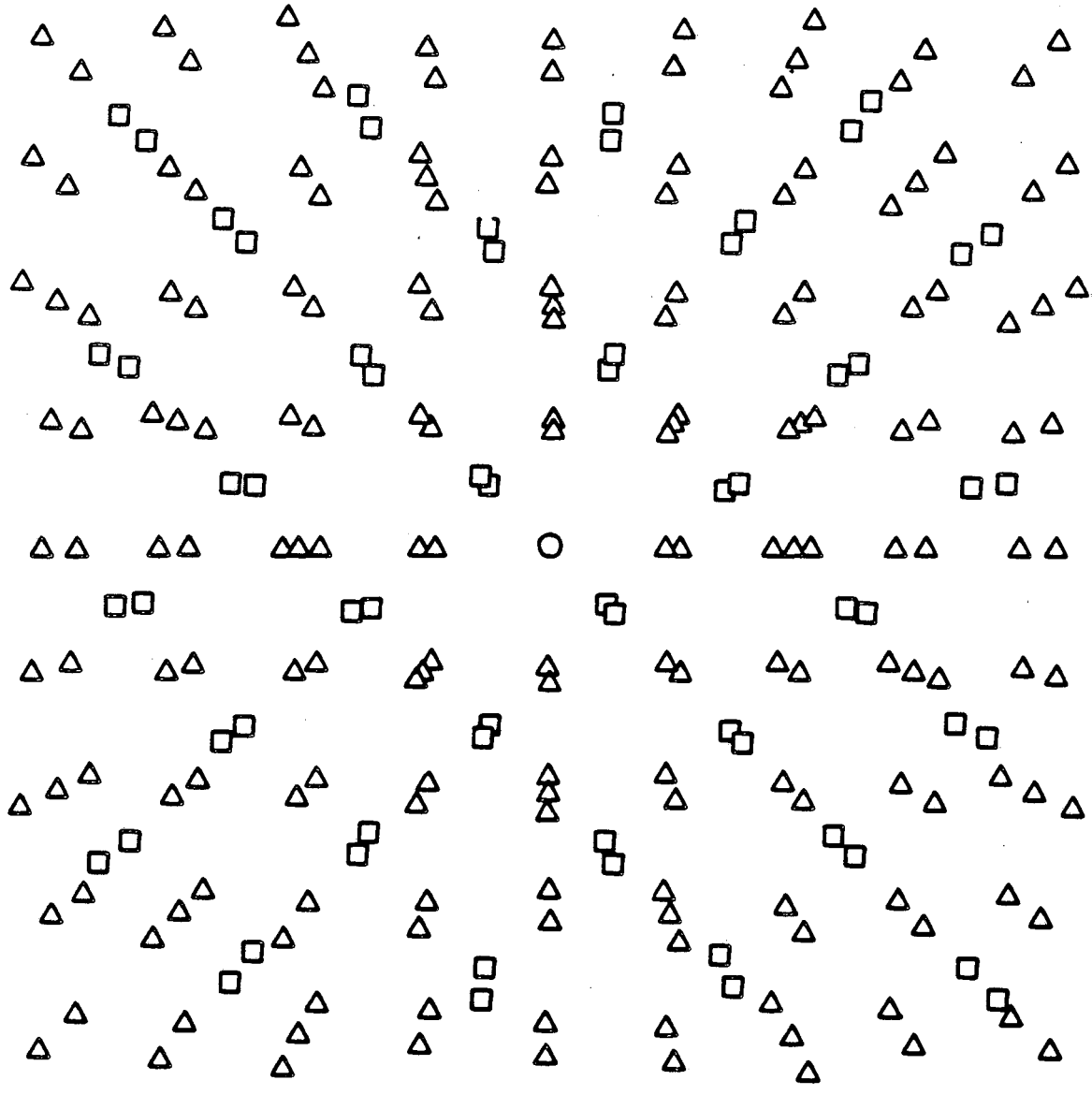

XBL 847-2866

Fig. 4

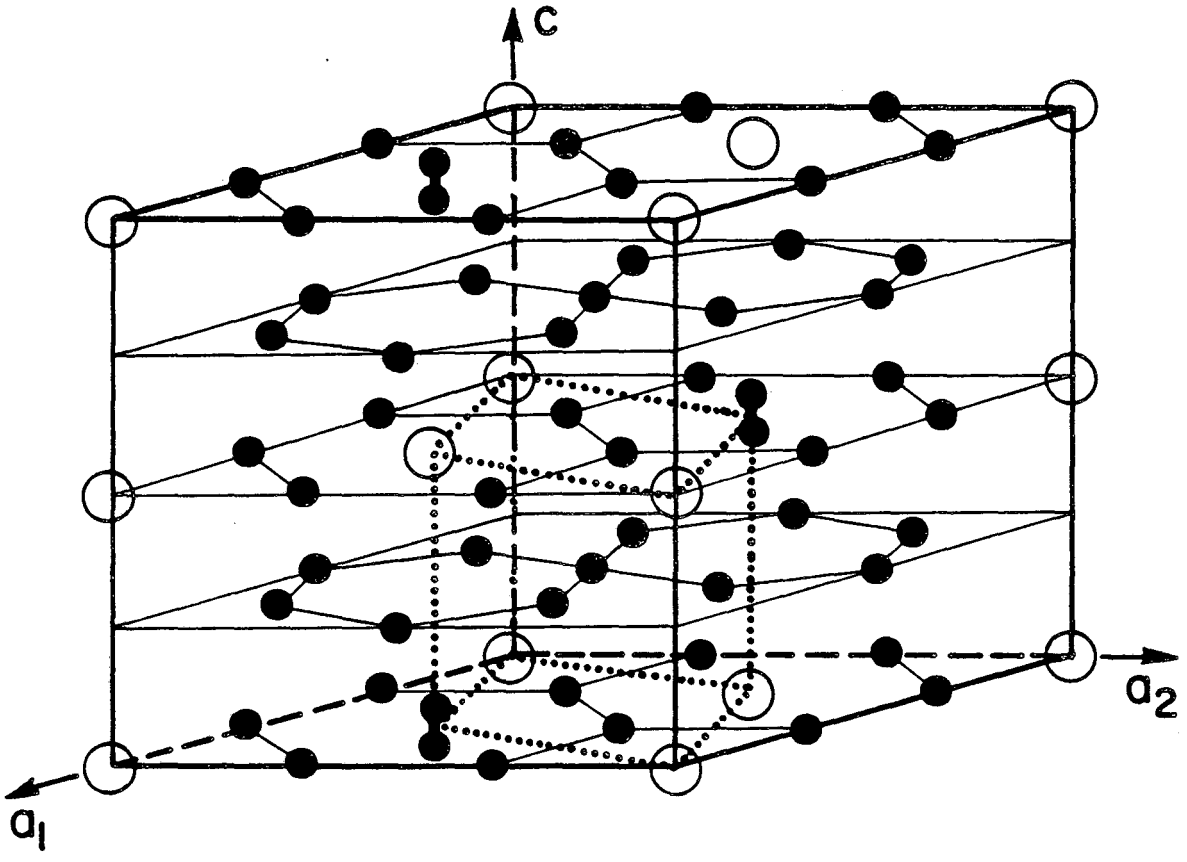

Hexagonal Sm_2Co_{17} Primitive Cell

○ Sm

● Co

XBL 831-5006

Fig. 5

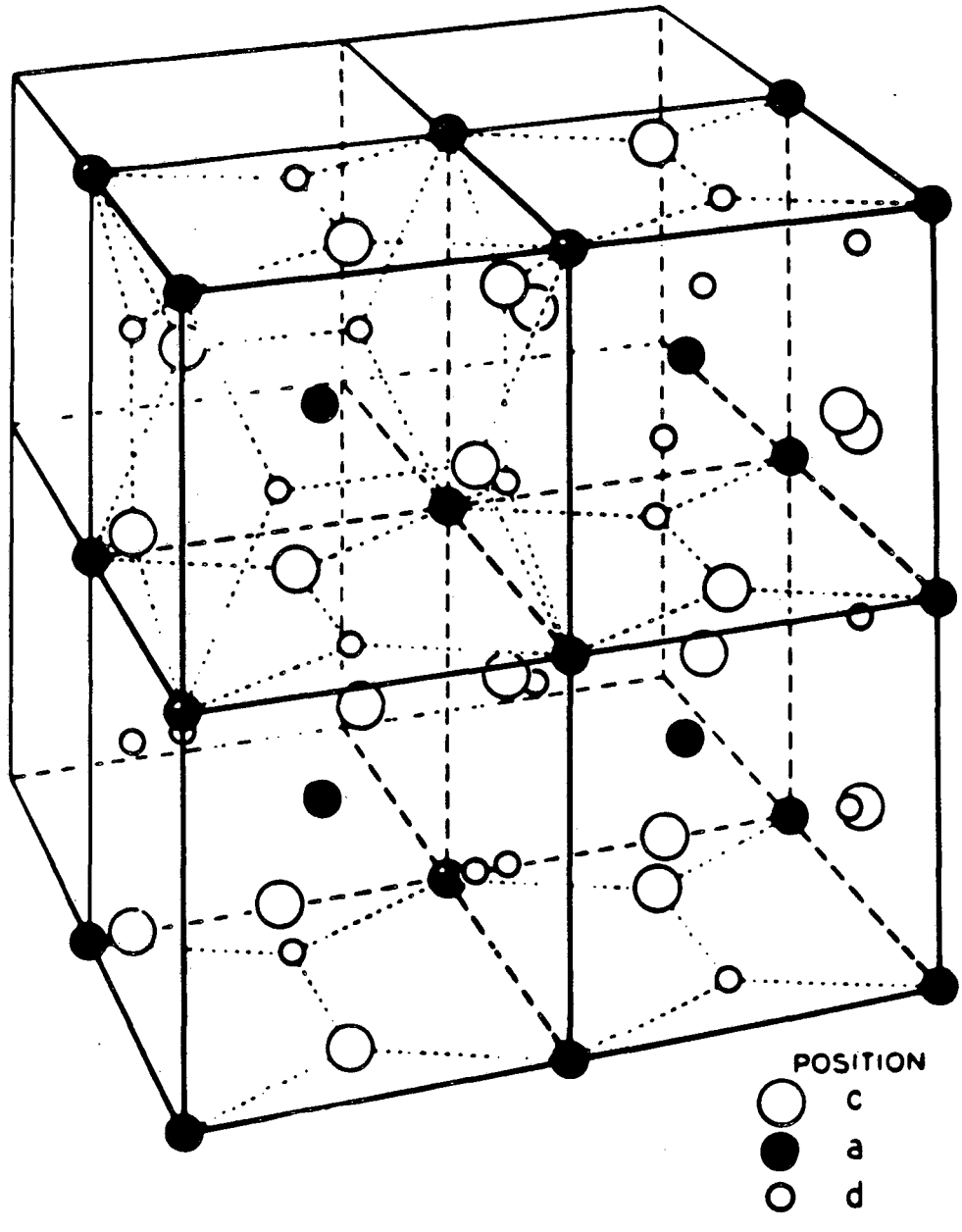

XBL 839-11350

Fig. 6

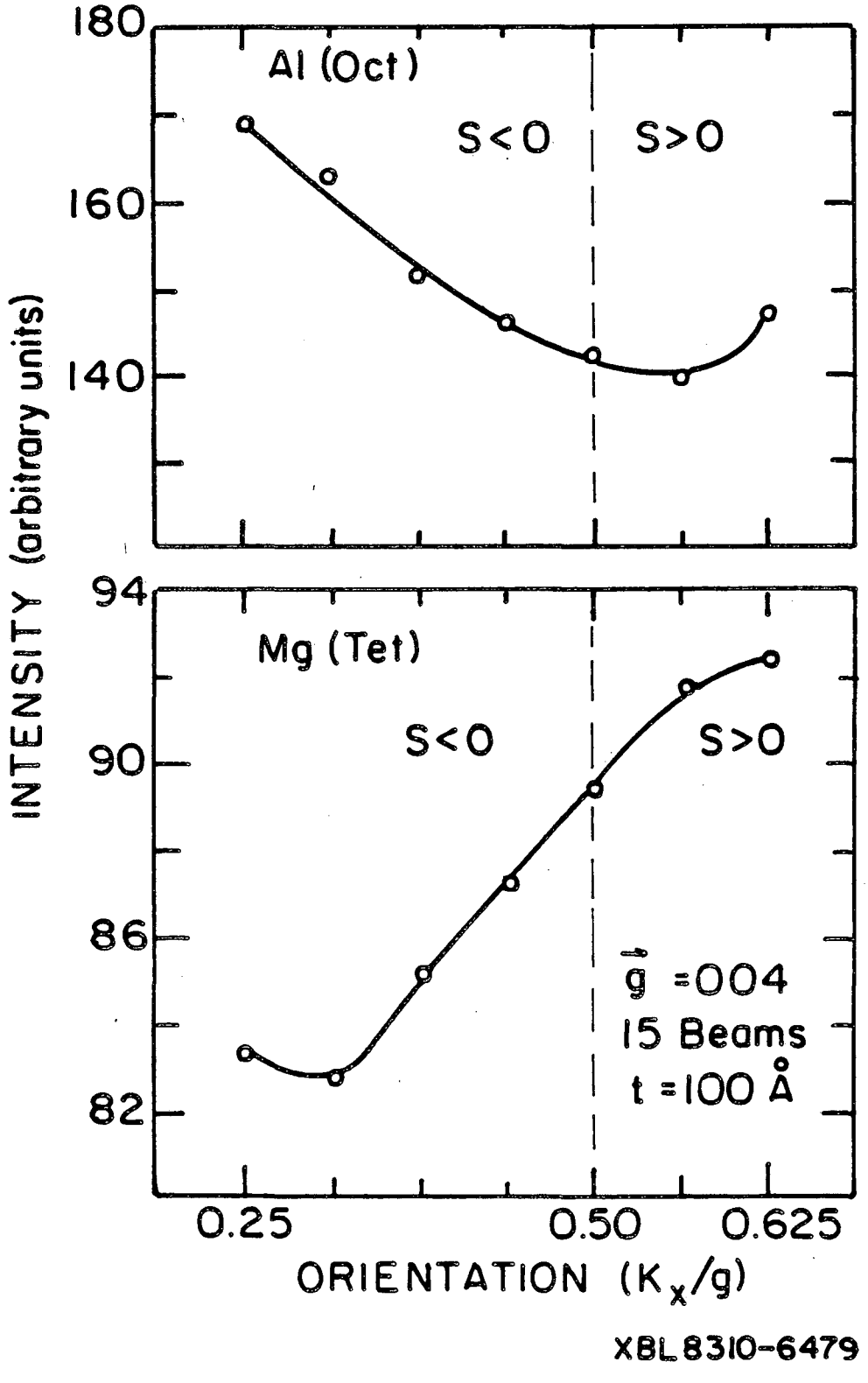
180
160
140
Al (Oct)
S<0
S>0
94
90
86
82
Mg (Tet)
S<0
S>0
$\vec{g}$ =004
15 Beams
t =100 Å
INTENSITY (arbitrary units)
0.25
0.50
0.625
ORIENTATION (K_x/g)
XBL8310-6479

Fig. 7(a)

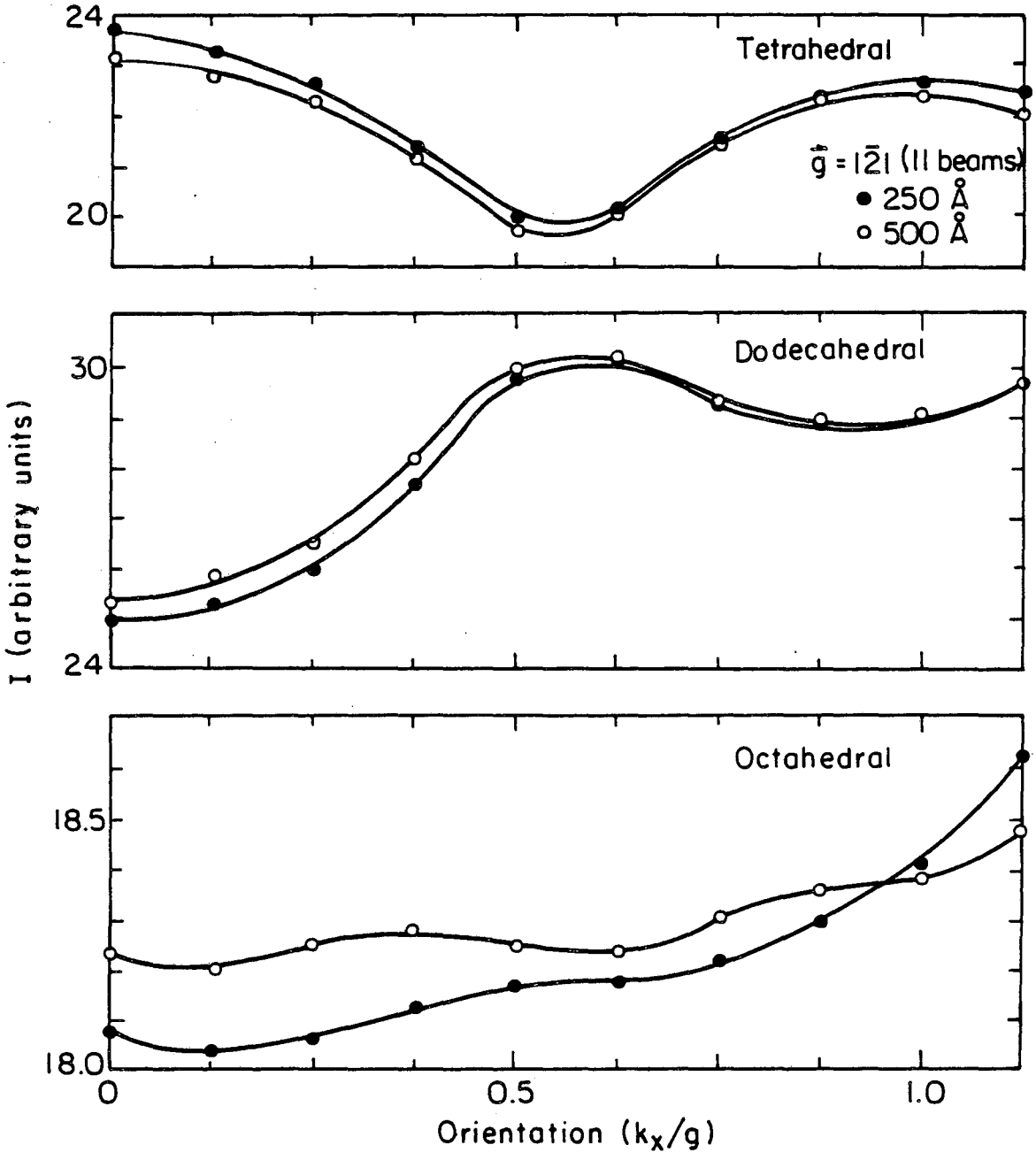

XBL 831-5156

Fig. 7(b)

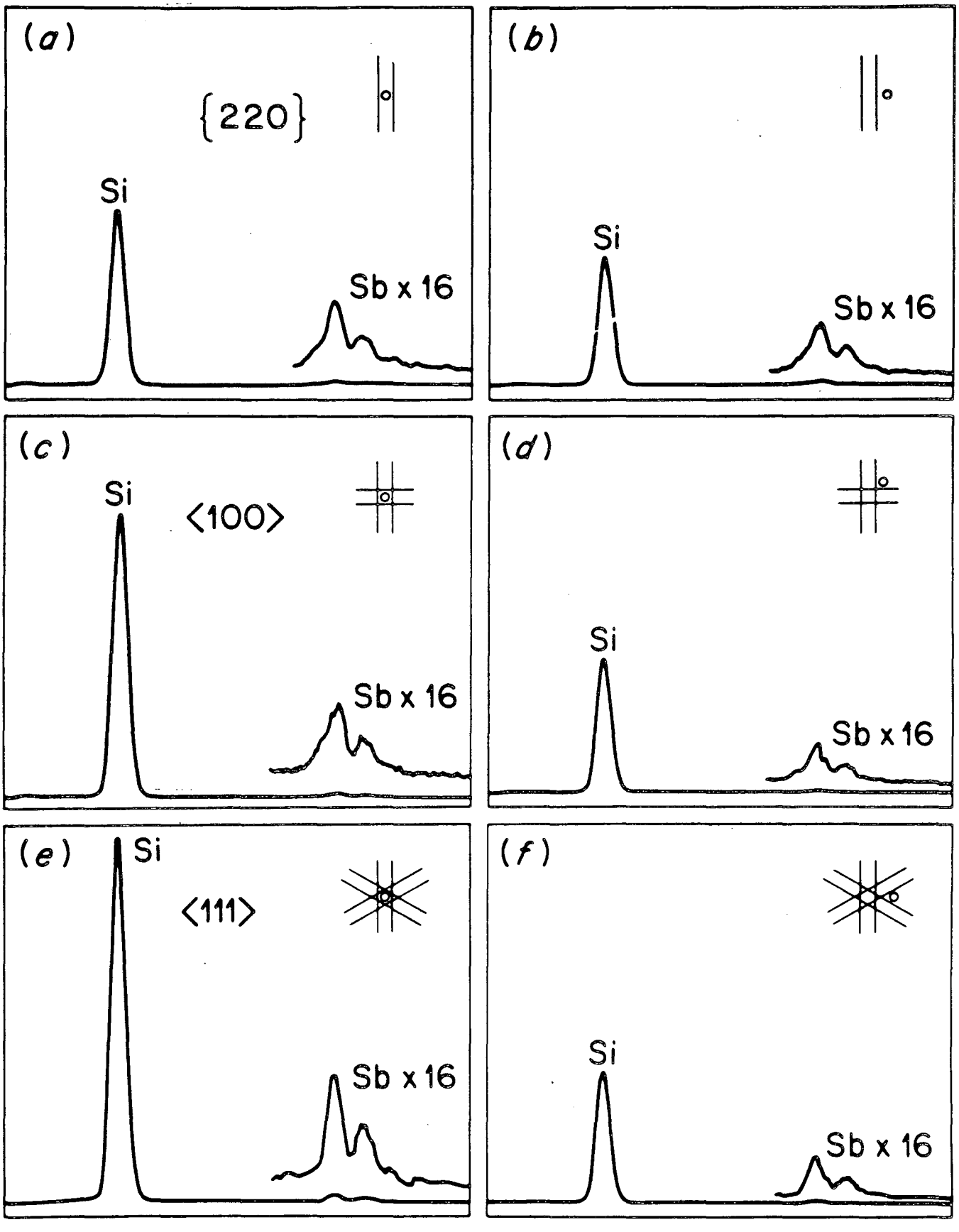

Fig. 8

XBL 8610-3784

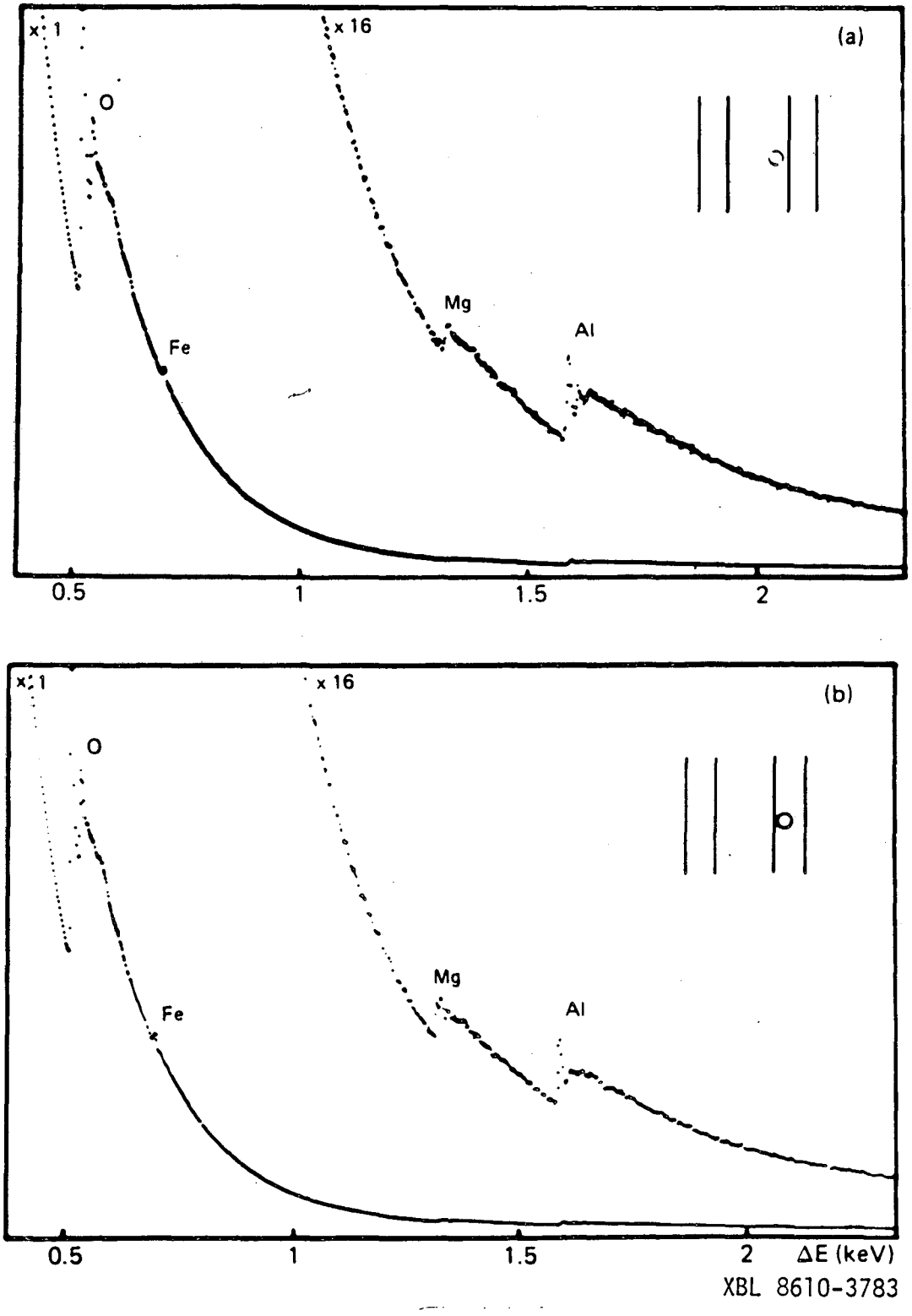
x 1
x 16
(a)
O
Mg
Al
Fe
0.5
1
1.5
2
x 1
x 16
(b)
O
Mg
Al
Fe
0.5
1
1.5
2
ΔE (keV)
XBL 8610-3783

Fig. 9

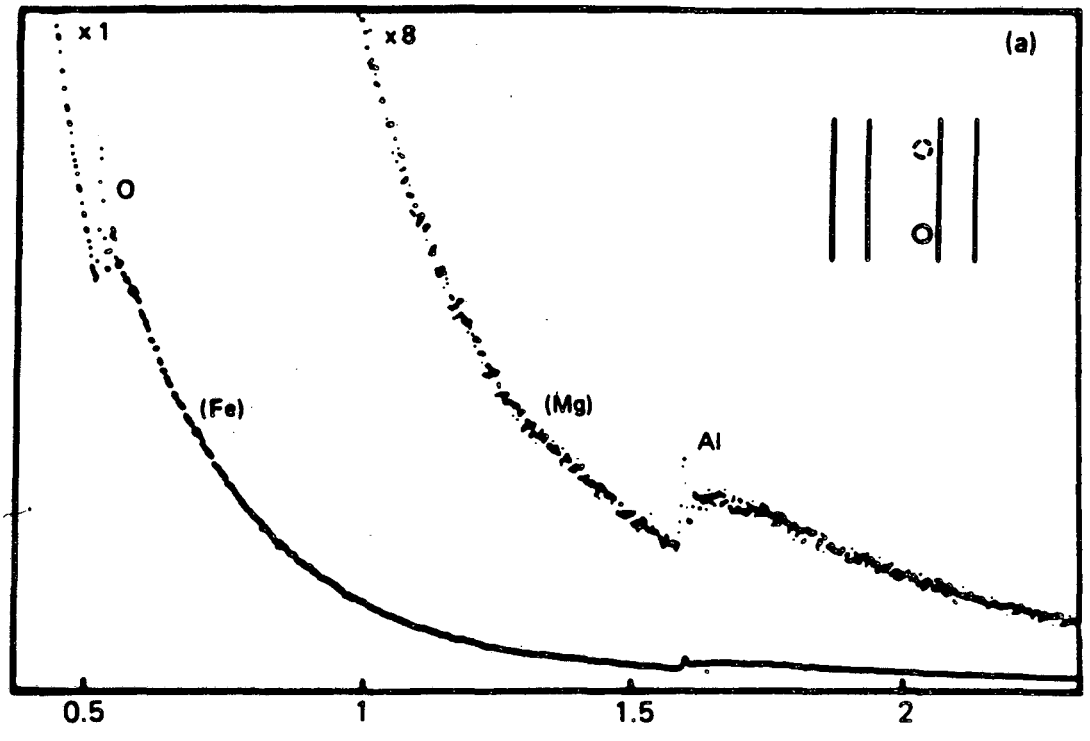

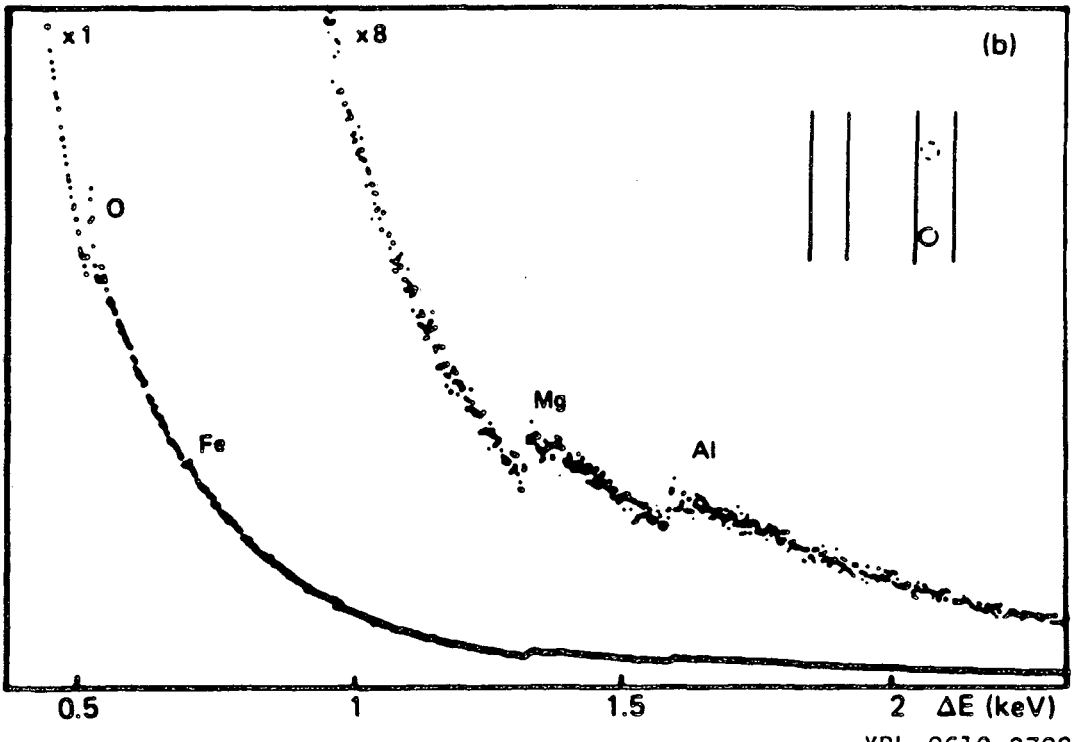

XBL 8610-3782

Fig. 10

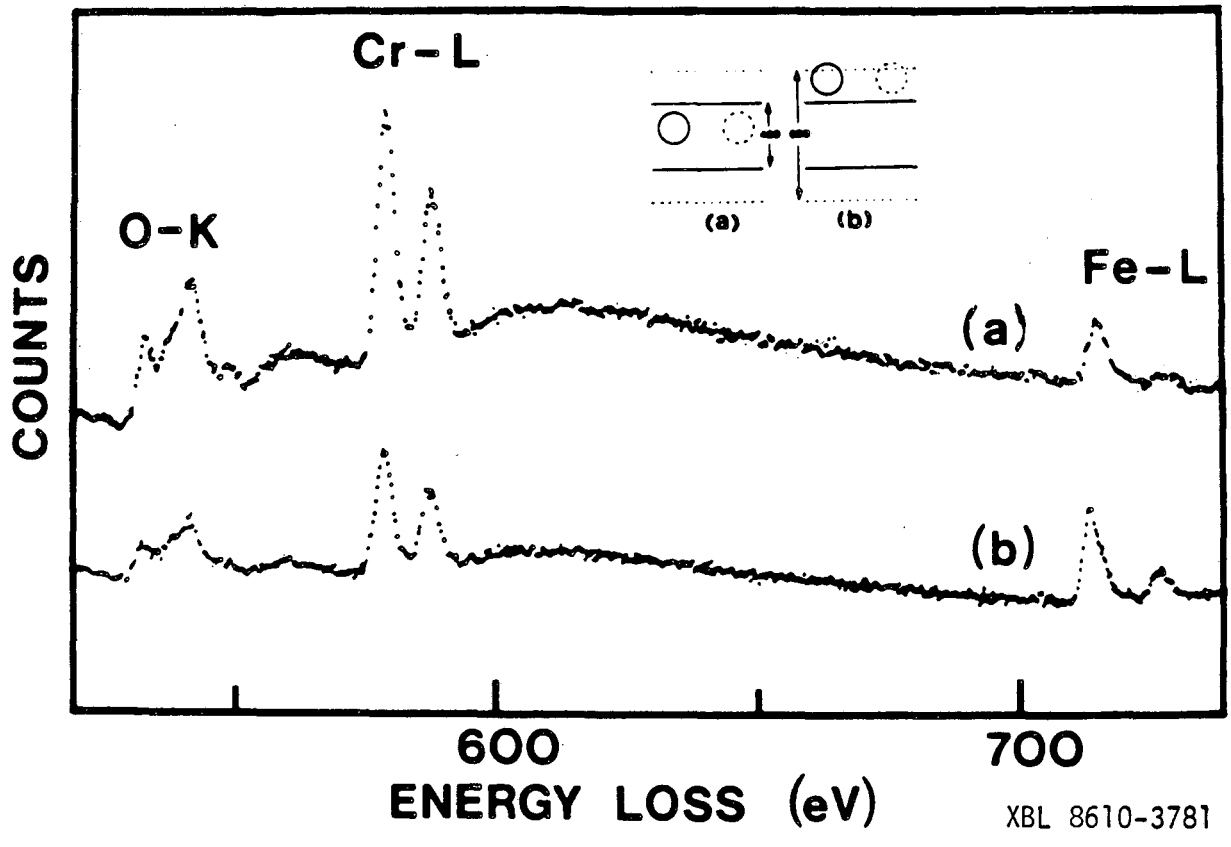

Fig. 11

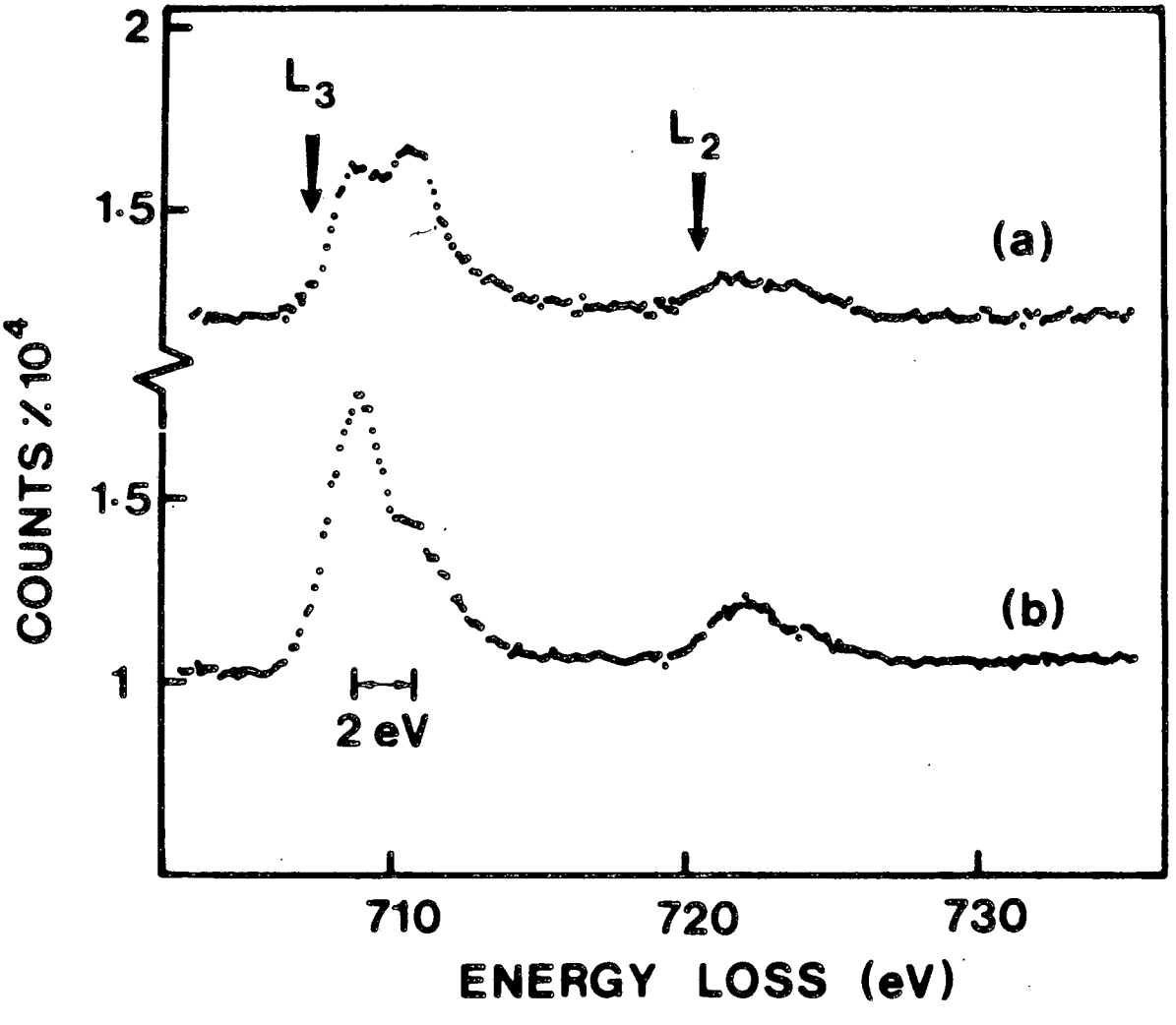

XBL 8610-3780

Fig. 12

LAWRENCE BERKELEY LABORATORY
TECHNICAL INFORMATION DEPARTMENT
UNIVERSITY OF CALIFORNIA
BERKELEY, CALIFORNIA 94720